Comparative lipidomic analyses reveal differences in lipid metabolism profiles between CL3 and CL53 *C. oleifera* cultivars

ABSTRACT: *Camellia oleifera* Abel. is an evergreen oil-bearing tree and widely cultivated in China. *Camellia oleifera oil* is considered to be a healthiest edible oil. However, the lipid profile are not well studied and ultilized. In the current study, we firstly used non-targeted LC-MS/MS method to describe the lipid profiles of two *C. oleifera* cultivars. Stringent criteria was used to screen significantly different lipids metabolites (SDLs). By comparing CL3 with CL5, 79 SDLs in CL3 were found to be significantly up-regulated, and 61 SDLs were found to be significantly down-regulated. Correlation analysis indicated that intra-category and inter-category correlation of glycerolipids and glycerophospholipids were strong in CL3 and CL53 cultivars. Through pathway enrichment analysis, we found that the most influential pathway in two cultivars was the glycerophospholipid metabolism pathway. The present results provide essential insights into lipid composition and a basis to make better ultilization of the lipids.

Keywords: *Camellia oleifera* Abel.; Lipids; Non-targeted LC-MS/MS; Lipid profile

1. INTRODUCTION

Camellia oleifera Abel., belonging to the genus *Camellia* of Theaceae, is an evergreen oil-bearing tree. Because of the high oil content in seeds and well adapted, hundreds of cultivars were worked out and cultivated widely in China. The plantation area has reached 4,443,300 hectares with a total output value of about 113.394 billion CNY in 2018 [1]. Changlin clones of *C. oleifera* have been studied by the Subtropical Forestry Research Center of Chinese Academy of Forestry Sciences for many years. After careful cultivation and selection by many scientific researchers, the cultivars including 'Changlin 3' (CL3) and 'Changlin 53' (CL53) with high quality and high yield were selected. In 2008, the CL3 and CL53 were approved as excellent caltivars of *C. oleifera* by Forest Variety Approval Committee of State Forestry Administration. The oil contents in kernels of CL3 and CL53 were 46.43% and 41.22%,

respectively [2]. The color of the fresh fruit of CL 3 is cyan yellow, and the shape is olive; The color of the fresh fruit of CL 53 is yellow red, and the shape is oblate (Fig. 1).

Camellia oleifera oil (Coo) is extracted from mature seeds of *C. oleifera* [3,4]. The composition of Coo is very similar to Olive oil [5]. It contains up to 93% unsaturated fatty acids, rich in bioactive substances, and is considered to be the healthiest edible oil [6]. As reported that increasing the amount of unsaturated fats intake, especially polyunsaturated fats, could help to decrease the risk of developing non-communicable diseases[7]. In China, Coo can be used not only as edible oil, but also as a health caring medicine to treat skin burns and infantile eczema as over-the-counter medicine [8]. The anti-inflammatory effect of Coo was confirmed to the phenolic compounds [9]. Four fractions of phenolic compounds and their in vitro anti-inflammatory activities had been quantitated and worked out, respectively [10]. In addition, the active ingredients in Coo had been proved to relieve liver fibrosis [11,12].

Lipids are a highly complex and diverse class of compounds and they can be classified into eight categories, glycerolipids (GLs), glycerophospholipids (GPs), sphingolipids (SPs), fatty acyls (FAs), prenol lipids (PRs), saccharolipids (SLs), sterol lipids (STs), and polyketides (PKs), according to their structural differences [13]. Lipids play an important role in biological processes including energy storage and conversion, material transports, signals recognition and transmission, cell development and differentiation [14]. EHA and DHA were reported to lower the risk of atherosclerosis [15]. Phospholipids are the main components of biological membranes[16]. Abnormal metabolism of GLs are related to the developing coronary heart disease [17], . The development of lipidmics technology provides convenience for us to understand lipids and their interrelatonships [14]. Indeed, several studies had utilized lipidomics technology for the elucidation of biological processes related questions [18-22]. In previous research, the fatty acids composition of Coo has always been the focus. Through comparative studies on the fatty acid composition between different clones or cultivars, the lipid characteristics was significantly affected by different clones or cultivars was concluded [23,24]. Therefore, understanding the lipid profile, breeding superior clones or cultivars with higher oil content and higher unsaturated fatty acids content of *C. oleifera* were considered to be very necessary.

In the current study, the fresh kernels of CL3 and CL53 at the mature stage were used as experimental materials. Non-targeted LC-MS/MS (liquid chromatography tandem mass spectrometry) method was used to analyze the lipid profiles of the fresh kernels of two *C. oleifera* cultivars for the first time. With the help of lipidomics analysis, more comprehensive lipids information will be clear. And this study can lay a solid foundation for the high value utilization of *C. oleifera*.

1. MATERIALS AND METHODS

1.1 Camellia oleifera cultivars sample collection

The mature fruits of *C. oleifera* CL3 and CL53 were collected from Huaguoshan farm in Liping County, Guizhou Province on 27th October, 2019. To minimize the biological differences, three biological duplications collected from each cultivar were analyzed. And each biological duplication was consist of the kernels which randomly selected from three fresh fruits with similar shape and size and maturity. These fresh kernels of a single fruit were taken out and put into a tube, then frozen with liquid nitrogen immediately. After back to lab, all samples were stored at -80□ until analyze.

1.2 Chemicals

The chemicals used in this study were as follows: water (7732-18-5; Thermon, USA), acetonitrile (75-05-8; Thermon, USA), methanol (67-56-1; Thermon, USA), isopropanol (67-63-0; Thermon, USA), dichloromethane (75-09-2; Scharlau, Spain), ammonium formate (540-69-2; SIGMA, USA).

1.3 Lipid extraction and quality control (QC) sample

The 100 mg of each sample was transferred to a tube, and then 500 μL of lysate (MeOH: H_2O=1:1) was added. The tissues were homogenized at 6500 mhz for 1 minute with Qiagen tissue analyzer and cycled three times. After the samples were incubated at -20 □ for overnight and then centrifuged at 13000 rpm, 4 □ for 20 min. The supernatant was discarded, and then added 5 mL of lysate (DCM: MeOH=3:1) and centrifuged at 13000 rpm, 4 □ for 20 min. The supernatant was dried and added mobile phase buffer B isopropanol (containing 5 mmol/L ammonium formate) in compound sample,

then centrifuged at 13000 rpm, 4 □ for 20 min. Quality control samples were equally mixed from lipid extracts of 60 samples from 20 cultivars including CL3 and CL53. Six identical QC samples were used to identify the lipids in C. oleifera and to ensure the reliability of the experimental results. Finally, the supernatant was analyzed by LC-MS/MS (ExionLCTM Series HPLC + SCIEX Triple-TOF 5600+).

1.4 Liquid-chromatography separation

Chromatographic analysis was performed using a ExionLCTM Series HPLC system. Samples were injected onto a kinetex 2.6 μm C18 100A (100×2.1mm, 2.6 μm) using a 20-min linear gradient at a flow rate of 0.3 mL/min. The mobile phase consisted of A (20% acetonitrile [ACN] + 60% H_2O + 20% methanol + 5 mM $HCOONH_4$), and B (5 mM $HCOONH_4$ + isopropanol). The solvent gradient was set as follows: 30% B, initial; 30% B, 1 min; 95% B, 14 min; 95% B, 17 min; 30% B, 17.1 min; 30%B, 20 min. The injection volumes were 2 μl for both positive- and negative-ion modes.

1.5 Mass spectrometric detection

Mass spectrometry was performed using a Triple-TOF 5600 (SCIEX, USA) with an electrospray ionization (ESI) source. In positive ion-mode (NT-pos), MS parameters were as follows: Curtain Gas: 35; Ion Spray Voltage: 5500; Temperature: 600; Ion Source Gas 1: 60； Ion Source Gas 2: 60; Collision energy: 40 eV. Acquisition was performed from Da 50 to 1200. In negative ion-mode (NT-neg), MS parameters were as follows: Curtain Gas: 35; Ion Spray Voltage: -4500; Temperature: 550; Ion Source Gas 1: 60; Ion Source Gas 2: 60; Collision energy: -40eV. Acquisition was performed from Da 50 to 1200.

1.6 Data processing for identification of lipids

The open-source software pipeline MS-DIAL (http://prime.psc.riken.jp/Metabolomics Software/) was wildly used for identification and quantification of small molecules by mass spectral deconvolution [32]. Raw data were transformed to an ABF file and then imported to the MS-DIAL for peak alignment to obtain a peak list containing the retention time (RT), mass to charge ratio(m/z), and peak

area of each sample. Database including LipidBlast was used for metabolites identification [33,34]. The mass error was set as 5 ppm. Metabolites' value of CV (Coefficient of Variance) in QC samples is less than 30% [35](Dai, W. et al 2017). In MS-DIAL, the quality collection range was set from 0 to 2000Da. In positive ion mode, the cutoff of matching score was set at 85. In negative ion mode, the matching score cutoff was set at 80.

1.7 Statistical analysis

For the high dimensions and correlations between variables of omics data, the potential informations cannot be mined quickly and accurately with traditional univariate analysis. Therefore, multivariate statistical methods, such as principal component analysis (PCA), partial least squares discriminant analysis (PLS-DA), should be used. PCA was performed to visualize a comprehensive clustering trend and outliers [36,37]. Principal component was conducted using SIMCA (Version 14.1, Umetrics, Sweden), and data were Log-transformed and Pareto-scaled. The square root of the standard deviation was used as the scaling factor [38]. The metaX packages of R language was used for PLS-DA analysis between CL3 and CL53 [39]. Based on the PLS-DA model, the corresponding variable importance in the projection (VIP values) was calculated. A sixfold cross-validation method was used to estimate the robustness and the predictive ability of our model. The 200 permutation tests were performed to verify whether the model was over-fitting [25]. Potential SDLs were selected with a VIP value >1, and a *P*-value of Student's t-test < 0.05. Data processing was conducted by Novogene Co., Ltd. (Beijing, China).

1.8 Correlation analysis

The hierarchical clustering analysis was generated using a scientific data analysis and visualization online tool (https://hiplot.com.cn/). The correlation network analysis was performed using Cytoscape 3.8.2 [40]. The lipid metabolism pathway analysis was performed using Web-based MetaboAnalyst (http://www.metaboanalyst.ca) [41].

2. RESULTS

2.1 Reliability of the analytical method

A total of 6 QC samples were added and tested before, during and after LC-MS/MS injection of the sample to be tested, respectively. The retention time and peak area of total ion chromatograms in QC samples were overlapped well in both positive and negative ion modes, indicating that instrument had excellent stability. As shown in PCA-X score plots, scores for all QC samples were distributed within two standard deviations, indicating that data were reliable [18]. In addition, QC samples with R2 >0.98 were highly correlated in both positive and negative ion modes, suggesting that data quality were sufficient. These results indicated the reliability of the analytical methods.

2.2 Lipids profiles of CL3 and CL53 samples

In total, 1329 lipid metabolites were identified according to the classification methods of MS-DIAL database . These metabolites can be summed up in 6 categories, namely 104 FAs, 547 GLs, 345 GPs, 286 SPs, 27 STs, 20 PRs. The 6 categories can be divided into 27 main class, including 32 fatty acids and conjugates [FA01], 13 fatty esters [FA07], 59 fatty amides [FA08], 20 isoprenoids [PR01],9 other sterol lipids [ST00], 14 sterols [ST01], 1 steroid conjugates[ST05], 22 sphingoid bases[SP01], 102 ceramides [SP02], 14 phosphosphingolipids [SP03], 101 neutral glycosphingolipids [SP05], 46 acidic glycosphingolipids [SP06], 48 other glycerophospholipids[GP00], 42 glycerophosphocholines [GP01], 58 glycerophosphoethanolamines [GP02], 14 glycerophosphoserines [GP03], 69 glycerophosphoglycerols [GP04], 49 glycerophosphoinositols [GP06], 51 glycerophosphates[GP10], 10 glycerophosphoglycerophosphoglycerols [GP12], 97 other glycerolipids [GL00], 10 monoradylglycerols [GL01], 133 diradylglycerols [GL02], 221 triradylglycerols [GL03], 86 glycosyldiradylglycerols [GL05] (Fig. 2A), and subdivided into 71 subclass, such as NAE, PMeOH, TG and etc. The GLs accounted for the largest proportion among the 6 categories, accounting for 41%. The GPs and SPs accounted for 26% and 22%, respectively, ranking second and third. FAs accounted for 8%. STs account for 2% and PRs account for 1% (Fig. 2B).

The relative abundance of each main class was estimated by the ratio of the sum of the relative concentration of the same main lipid to that of the total lipid. When CL3 was compared with CL53, the relative abundances of GL02, GL03, SP05, FA08 were increased, but the relative abundance of GL00 and SP02 were decreased with NT-pos mode. The relative abundance of GP10 and GP02 increased, but GP00, GP06 decreased with NT-neg mode (Fig. 3A and 3B). Both in CL3 and CL53 the GL, GP categories account for most.

2.3 Identification of significantly different lipids metabolites (SDLs) between CL3 and CL53

Comparison between CL3 and CL53 groups with regard to the lipid components was performed by PCA and PLS-DA analyses. The PCA in NT-pos and in NT-neg was showed in Fig. 4A and 4B. The cumulative proportion for PC1 (explained variation 58.1%) and PC2 (21.3%) was 79.4% in NT-pos (Fig. 4A). The cumulative proportion for PC1 (explained variation 70.3%) and PC2 (13.0%) was 83.3% in NT-neg (Fig. 4B). The CL3 and CL53 had good separation on principal component 1, and the samples all in 95% confidence intervals (Fig. 4A and 4B), indicating that CL53 and CL3 had a very distinct lipid composition and no outliers. The PLS-DA score showed that all samples were well differentiated under NT-pos and NT-neg conditions (Fig. 4C, 4D). The R2Y>Q2Y>0.5 indicated that the model had excellent interpretability and predictability. The PLS-DA permutation plots (Fig. 4E, 4F) were used for effectively assessing whether the current PLS-DA model was over-fitting. Any one of the following criteria needed to be satisfied. Firstly, all Q2 points were lower than the rightmost original Q2 point. Secondly, the regression line of the Q2 point was less than or equal to zero at the intersection of the ordinate [25]. The Q2 intercept was less than zero, indicating the model was not over-fitting [26]. The PLS-DA model also provided the VIP score, which was a measure of a variable's importance in the analysis. In summary, the model could effectively distinguish the features of two groups. Furthermore, the threshold for screening SDLs was narrowed as follows: $P < 0.05$, $VIP > 1.0$.

With the above criteria, 140 SDLs were identified between CL53 and CL3, 74 in NT-pos and 66 in NT-neg, finally. By comparing CL3 with CL53, 79 SDLs in CL3 were found to be significantly up-regulated, and 61 SDLs were found to be significantly down-regulated. To better visualize these differ-

ences, the hierarchical analysis was conducted using Euclidean distance with an average clustering algorithm [27]. A heat map with dendrograms showing the hierarchical clustering of SDLs was generated. When CL3 compared with CL53, the DGGA and DGTS/A subclasses of GL00 main class, LPI and PI subclass of GP06 main class, PEtOH and PMeOH subclasses of GP00 main class, and ST subclass of ST01main class were almost all significantly down-regulated among the140 SDLs. However, the DGDG subclass of GL05 main class, TG and EtherTG of GL03 main class, LPC and PC subclasses of GP01 main class, VAE subclass of PR01 main class, Cer and Cer-NS of SP02 main class were nearly all up-regulated (Fig. 5A ,5B).

2.4 Correlation analysis of SDLs between CL3 and CL53

Owing to numerous lipids have similar physiological and molecular characteristics, and the same trend at mature stage, the hypothesized that they were correlated/co-regulated was valid. To assess this, an unweighted correlation network analysis of 140 SDLs was performed to reveal interactions among different lipid species and classes. As shown in Fig. 6, numerous lipids were highly correlated. In total, 272 correlations were detected in the CL3 group, and 269 correlations in the CL53 group (*P*-value < 0.05). Among these SDLs, intra-category and inter-category correlation of GL and GP were strong in CL3 and CL53. However, intra-category correlations of GP, SP, FA, ST and PR were relatively weak. These results indicated that different categories of lipids were related, and GL had strong intra-category and inter-category correlation with other categories during the oil accumulation at mature stage.

2.5 Metabolic pathways of SDLs analysis

To further explore the effects of these SDLs, we performed a pathway analysis using pathway analysis model of MetaboAnalyst 5.0. The 140 SDLs were mapped to the KEGG, HMDB, and PubChem databases. In total, 7 metabolic pathways were obtained when SDLs were searched against the KEGG pathway database in Arabidopsis thaliana library. The *P*-value and pathway impact were calculated from pathway topology analysis, respectively. The most relevant pathways identified were glycerophospholipid metabolism, glycerolipid metabolism, glycosylphosphatidylinositol (GPI)-anchor bio-

synthesis. Linoleic acid metabolism, arachidonic acid metabolism, phosphatidylinositol signaling system, alpha-linolenic acid metabolism had little pathway impact (Fig. 7A). Among these, glycerophospholipid metabolism pathway was the most significantly relevant metabolic pathway.

3. DISCUSSION

Coo is a complex and heterogeneous mixture containing thousands of lipids. The present results deepened our understanding of the lipids composition of Coo. Comparison with traditional methods, high-throughput lipidomics can simultaneously identify and quantify hundreds of lipids, including polar and non-polar, high-abundance and low-abundance lipids. Previously, gas chromatography was used to determine the fatty acid composition of different *C. oleifera* cultivars, and the composition of triglycerides were analyzed in Coo by high performance liquid chromatography (HILIC) [28]. In this study, using the LC-MS/MS method, 1329 lipids of 27 main classes and 140 SDLs were identified in CL3 and CL53. Futhermore, we have a more comprehensive understanding of the lipid composition in the fresh kernels of *C. oleifera* at mature stage, which provides a basis for us to make better ultilization of the lipids in Coo. At the same time, it also provides a valuable information for cultivars breeding.

In the present study, we found that the composition types of lipids contained in the mature fresh kernels of CL3 were consistent with that in CL53. The 1329 identified lipids was detected in CL3 and CL53. It may be caused by the similar genetic backgrounds of CL3 and CL53. However, the relative abundance of different lipid classes in CL3 and CL53 was different, indicating that the concentration of different lipid classes in different varieties was different. The main storage form of plant oil was triacylglycerol (TAG) ,which was a glycerol skeleton on which three fatty acids were esterified in sequences. The synthesis and assembly of TAG in plants is complicated. After fatty acids are located in the endoplasmic reticulum, they are assembled into TAG through the combination of two pathways. One is that diacylglycerol acyltransferases (DGAT) transfer acyl-CoAs to the sn-3 position of DAG to produce TAG. The other is that phospho-lipid: diacylglycerol acyltransferases (PDAT) transfer the sn-2 acyl group of phospholipids to DAG to form TAG. [20,29-31]. Through the operation of DGAT and/or PDAT, any PC-derived DAG generated by these activities can be assembled into TAG [29-31]. In CL3

and CL53, the number of GLs accounted for 41% of all lipids, and GPs accounted for 26%. In NT-pos mode, the contents of GLs were the highest, accounting for 80% of the total lipids. The total lipid contents of GL03 in CL3 and CL53 were 38.74% and 31.78%, respectively. The total lipid contents of GL02 in CL3 and CL53 were 27.22%, and 23.31%, respectively. In NT-neg mode, the contents of GPs were the highest, accounting for 75% of the total lipids. The total lipid contents of GP10 in CL3 and CL53 were 48.49%%, and 39.06%, respectively (Fig. 3C, 3D). GLs and GPs categories regardless of the proportion of the number of lipids types or the proportion of relative concentration was more dominant than other types of lipids. In addition, we found that in the CL53, the number of GLs category in the SDLs had 216 correlation network edges, and an average of 3.93 SDLs had a strong correlation with the GLs of SDLs. However, in the CL3, there were 244 correlation network edges, and an average of 4.20 SDLs were strongly correlated with the number of GLs category of SDLs. Furthermore, The SDLs correlation network of CL3 was more complicated than that of CL53. CL3 was divided into 8 clusters (Fig. 6A), and CL53 was divided into 7 clusters (Fig. 6B). We speculate that there are more SDLs in CL3 that transform to GLs category, and a storage of oil was carried out. At the same time, the fact that the oil production characteristics of CL3 were better than CL53. That also supports our findings. At the mature stage, fatty acid synthesis will transform to triacylglycerol (TAG). Although the structure of some basic pathways for fatty acid and lipid synthesis in plants has been well characterized, the enzymes in these pathways are little known about the regulations and working mechanisms. There are few studies on whether these enzymes work in specific crops. Therefore, it is necessary to elucidate the mechanism of these enzymes in the process of oil synthesis and transformation in *C. oleifera* fruits.

Through pathway enrichment analysis, we found that the most influential pathway between these two cultivars was the glycerophospholipid metabolism pathway. In the glycerophospholipid metabolism pathway, the network relationship of these different metabolites was shown in Fig. 7 B. The C04230 compound (LPC 18:1) and C00157 compounds (PC (16:0/18:0), PC (16:0/18:3)) can be inversely transformed. The C00157compounds (PC (16:0/18:0), PC (16:0/18:3)), and C00350 compound (PE 44:6) can be transformed into C00416 compounds (LPA (18:0), LPA (18:1)). The CL3 expression

level of these metabolites in the network was higher than that of CL53. We speculated that there were differences in the activity of certain enzymes that regulated the metabolic network in CL3 varieties. For example, in the process of the transition from C00157 to C00416 and C00350 to C00416, the phospholipase D1/2 was required to participate in phosphatidylcholine phosphatidyl hydrolysis reaction , since the expression intensity of the gene encoding phospholipase D1/2 in CL3 may be higher than that of CL53.

Since *C. oleifera* lacks genome-wide data, it is a feasible way to analyze possible causes of lipid differences in different cultivars of *C. oleifera* using multi-omics techniques. In addition, although a large number of lipid metabolites have been identified, how the mutual transformation of different lipids is still unknown. Huge number of lipid metabolites have not been matched to the pathway in the KEGG database. Therefore, it is complicated for *C. oleifera* and the study of lipid metabolism pathway still needs further work. This research can fill the gap in the lipid profiles of *C. oleifera*, and also provide a reference for the subsequent analysis of the complex mechanism of the lipid synthesis. At the same time, this research can provide a basis for us to make better ultilization of the lipids in Coo.

4. CONCLUSIONS

In the current study, lipids in mature kernels of *C. oleifera* were characterized using a non-target LC-MS/MS approach. In total, 140 SDLs were selected from 1329 lipids assigned to 6 categories, 27main class, 71 subclass in CL3 and CL53. Furthermore, the correlations and the related metabolic pathways of these 140 SDLs were analyzed. Seven metabolic pathways associated with changes in lipids were detected. The most significant pathway of which was glycerophospholipids metabolism, and followed by the glycerolipid metabolism, glycosylphosphatidylinositol (GPI)-anchor biosynthesis metabolism. Our research results in the present study can fill the gap in the lipid composition of *C. oleifera*, and also provide a reference for the subsequent analysis of the complex mechanism of the lipid synthesis of *C. oleifera* by the combination of multi-omics technology. We speculate that the reason for the difference in glycerophospholipid metabolism between CL3 and CL53 may be related to some enzymes activity such as phospholipase activity between these two cultivars.

Our results provided a basis for a comprehensive understanding of the lipid characteristics of *C. oleifera* fruit at the mature stage and a deeply understanding of the lipid differences between two *C. oleifera* cultivars in the 'Changlin' clones. It will also provide practical and important references for the breeding and development of *C. oleifera* varieties.

COMPETING INTERESTS

Authors have declared that no competing interests exist.

REFERENCES

1. Yu, S.H.; Zeng, Z.; Fu, W.Y.; Xiong, X.; Liu, Y.; Tan, X.F.; Wang, Z.R.; Song, J.Q. Status analysis and countermeasures of high quality development of oil tea industry in Hunan. *Nonwood For. Res.* **2019**, 37, 214-220 (in Chinese). https://doi.org/10.14067/j.cnki.1003-8981.2019.04.030
2. Xu, Y.; Li, B.G.; Wang, S.; Zhong, Q.P. Study on the correlation between some botanical characters and oil yield of Changlin clones of *Camellia oleifera*. *Forest Sci. Technol.* **2010**, 19, 143-153 (in Chinese). https://doi.org/10.13456/j.cnki.lykt.2010.04.024
3. Zhang, D.S.; Jin, Q.Z.; Wang, X.G.; Xue, Y.L. Research status of nutrition quality of *Camellia oleifera* seed and oil. *Sc. Technol. Cereals* **2013**, 21, 53-56 (in Chinese). https://doi.org/10.16210/j.cnki.1007-7561.2013.04.012
4. Yang, C.; Liu, X.; Chen, Z.; Lin, Y.; Wang, S. Comparison of oil content and fatty acid profile of ten new *Camellia oleifera* cultivars. *J. Lipids* **2016**, 3982486. https://doi.org/10.1155/2016/3982486
5. Ma, J.; Ye, H.; Rui, Y.; Chen, G.; Zhang, N. Fatty acid composition of *Camellia oleifera* oil. *J. Verbr. Lebensm.* **2011**; 6, 9-12.
6. Ke C. The main nutrient composition and health function of tea oil. *Modern Food.* **2019**, (13), 105-108 (in Chinese). https://doi.org/10.16736/j.cnki.cn41-1434/ts.2019.13.033
7. Healthy Diet. https://www.who.int/en/news-room/fact-sheets/detail/healthy-diet (**2018)**.
8. Wu, X.H.; Huang, Y.F.; Xie, Z.F.; Health functions and prospective of *Camellia* oil. *Food Sci. Technol.* **2005**, (8), 94-96 (in Chinese). https://doi.org/10.13684/j.cnki.spkj.2005.08.029
9. Chang, M.; Qiu, F.; Lan, N.; Zhang, T.; Guo, X.; Jin, Q.; L, R,;Wangl, X. Analysis of phytochemical composition of *Camellia oleifera* oil and evaluation of its anti-inflammatory effect in lipopolysaccharide-stimulated RAW 264.7 macrophages. *Lipids* **2020**, 55, 353-363. https://doi.org/10.1002/lipd.12241
10. Zhang, T.; Qiu, F.; Chen, L.; Liu, R.; Chang, M.; Wang, X. Identification and in vitro anti-inflammatory activity of different forms of phenolic compounds in *Camellia oleifera* oil. *Food Chem.* **2021**, 334, 12660. https://doi.org/10.1016/j.foodchem.2020.128660
11. Cheng, Y.T.; Lu, C.C.; Yen, G.C. Beneficial effects of *Camellia* oil (*Camellia oleifera* Abel.) on hepatoprotective and gastroprotective activities. *J. Nutr. Sci. Vitaminol.* **2015**, 61 Suppl(Supplement), S100-S102. https://doi.org/10.3177/jnsv.61.S100

12. Lei, X.; Liu, Q.; Liu, Q.; Cao, Z.; Zhang, J.; Kuang, T.; Fang, Y.; Liu, G.; Qian, K.; Fu, J.; et al. *Camellia* oil (*Camellia oleifera* Abel.) attenuates CCl_4-induced liver fibrosis via suppressing hepatocyte apoptosis in mice. *Food Funct.* **2020**, 11, 4582-4590. https://doi.org/10.1039/c9fo02258a
13. Fahy, E.; Subramaniam, S.; Brown, H.A.; Glass, C.K.; Merrill, A.H.; Murphy, R.C.; Raetz, C.R.H.; Russell, D.W.; Meer, G.V.; Shaw, W.; et al. A comprehensive classification system for lipids. *J. Lipid Res.* **2005**, 46, 839-861. https://doi.org/10.1194/jlr.E400004-JLR200
14. Cai, T.X.; Liu, P.S.; Yang, F.Q.; Yang, F.Y. The research advances in the field of lipidomics. *Prog. Biochem. Biophys.* **2010**, 37(2), 121-128 (in Chinese).
15. Steffens, W. Aquaculture produces wholesome food: Cultured fish as a valuable source of n-3 fatty acids. *Aquacult. Int.* **2016**, 24, 787−802. https://doi.org/10.1007/s10499-015-9885-8
16. Hou, Q.; Ufer, G.; Bartels, D. Lipid signalling in plant responses to abiotic stress. *Plant Cell Environ.* **2016**, 39, 1029−1048. https://doi.org/10.1111/pce.12666
17. Qin, M.; Zhu, Q.; Lai, W.; Ma, Q.; Liu, C.; Chen, X.; Zhang, Y.; Wang, Z.; Chen, H.; Yan H.; et al. Insights into the prognosis of lipidomic dysregulation for death risk in patients with coronary artery disease. *Clin. Transl. Med.* **2020**, 10, e189. https://doi.org/10.1002/ctm2.189
18. Li, M.; Li, Q.; Kang, S.; Cao, X.; Zheng, Y.; Wu, J.; Wu, R.; Shao J.; Yang M.; Yue X. Characterization and comparison of lipids in bovine colostrum and mature milk based on UHPLC-QTOF-MS lipidomics. *Food Res. Int.* **2020**, 136, 109490. https://doi.org/10.1016/j.foodres.2020.109490
19. Liu, Y.; Jiao, J.G.; Gao, S.; Ning, L.J.; Limbu, S.M.; Qiao, F.; Chen, L.Q.; Zahng, M.L.; Du, Z.Y. et al. Dietary oils modify lipid molecules and nutritional value of fillet in Nile tilapia: A deep lipidomics analysis. *Food Chem*. **2019**, 277, 515-523. https://doi.org/10.1016/j.foodchem.2018.11.020
20. Woodfield, F.K.; Cazenave-Gassiot, A.; Haslam, R.P.; Guschina, I.A.; Wenk, M.R.; Harwood, J.L. Using lipidomics to reveal details of lipid accumulation in developing seeds from oilseed rape (*Brassica napus* L.). *BBA-Mol. Cell Biol. Lipids* **2018**, 1863, 339-348. https://doi.org/10.1016/j.bbalip.2017.12.010
21. Li, X.; He, Q.; Hou, H.; Zhang, S.; Zhang, X.; Zhang, Y., Wang, X.; Han, L.; Liu, K. Targeted lipidomics profiling of marine phospholipids from different resources by UPLC-Q-Exactive Orbitrap/MS approach. *J. Chromatogr. B* **2018**, 1096, 107-112. https://doi.org/10.1016/j.jchromb.2018.08.018
22. Ortega, A.; Mourente, G. Comparison of the lipid profiles from wild caught eggs and unfed larvae of two scombroid fish: northern bluefin tuna (*Thunnus thynnus* L. 1758) and Atlantic bonito (*Sarda sarda* Bloch, 1793). *Fish Physiol. Biochem.* **2010**, 36, 461-471. https://doi.org/10.1007/s10695-009-9316-8
23. Guo, X.L.; Xiao, P.; Du, S.G.; Luo, L.P.; Fu, Y.X. Fatty acid composition of *Camellia oleifera* Abel. seeds with different strains. *J. Nanchang U: Nat. Sci.* **2013**, 37(1), 43-46 (in Chinese).
24. Zeng, W.; Endo, Y. Effects of cultivars and geography in China on the lipid characteristics of *Camellia oleifera* seeds. *J. Oleo Sci.* **2019**, 68, 1051-1061.
25. Yuan, M.; Breitkopf, S.B.; Yang, X.; Asara, J.W. A positive/negative ion-switching, targeted mass spectrometry-based metabolomics platform for bodily fluids, cells, and fresh and fixed tissue. *Nat. protoc.* **2012**, 7, 872-881. https://doi.org/10.1038/nprot.2012.024
26. Zhang, Y.; Chen, W.; Chen, H.; Zhong, Q.; Yun, Y.; Chen, W. Metabolomics analysis of the deterioration mechanism and storage time limit of tender coconut water during storage. *Foods* **2020**, 9, 46. https://doi.org/10.3390/foods9010046
27. Liu, L.L.; Lin, Y.; Chen, W.; Tong, M.L.; Luo, X.; Lin, L.R.; Zhang, H.L.; Yan, J.H.; Niu, J.J.; Yang T.C. Metabolite profiles of the cerebrospinal fluid in neurosyphilis patients determined by untargeted metabolomics analysis. *Front. Neurosci.* **2019**, 13. https://doi.org/10.3389/fnins.2019.00150

28. Chen, B.L. Research on the oil quality characteristics of *Camellia oleifera* in southern belt, Central South University of Forestry and Technology, Changsha, Hunan, China, **2018**.
29. Bates, P.D.; Browse, J. The pathway of triacylglycerol synthesis through phosphatidylcholine in *Arabidopsis* produces a bottle neck for the accumulation of unusual fatty acids in transgenic seeds. *Plant J.* **2011**, 68, 387-399. https://doi.org/10.1111/j.1365-313X.2011.04693.x
30. Lu, C.; Xin, Z.; Ren, Z.; Miquel, M.; Browse, J. An enzyme regulating triacylglycerol composition is encoded by the ROD1 gene of *Arabidopsis*. *Proc. Nat. Acad. Sci. USA* 2009, 106, 18837-18842. https://doi.org/10.1073/pnas.0908848106
31. Haslam, R.P.; Sayanova, O.; Kim, H.J.; Cahoon, E.B.; Napier, J.A. Synthetic redesign of plant lipid metabolism. *Plant J.* **2016**, 87, 76-86. https://doi.org/10.1111/tpj.13172
32. Tsugawa, H.; Cajka, T.; Kind, T.; Ma, Y.; Higgins, B.; Ikeda, K.; Kanazawa, M.; VanderGheynst, J.; Fiehn, O.; Arita, M. MS-DIAL: data-independent MS/MS deconvolution for comprehensive metabolome analysis. *Nat. Methods* **2015**, 12, 523-526. https://doi.org/10.1038/nmeth.3393
33. Kind, T.; Okazaki, Y.; Saito, K.; Fiehn, O. LipidBlast templates as flexible tools for creating new in-silico tandem mass spectral libraries. *Anal. chem*. **2014**, 86, 11024-11027. https://doi.org/10.1021/ac502511a
34. Kind, T.; Tsugawa, H.; Cajka, T.; Ma, Y.; Lai, Z.; Mehta, S.S.; Wohlgemuth, G.; Barupal, D.K.; Showalter, M.R.; Arita, M.; et al. Identification of small molecules using accurate mass MS/MS search. *Mass Spectrom. Rev.* **2017**, 37, 513-532. https://doi.org/10.1002/mas.21535
35. Dai, W.; Xie, D.; Lu, M.; Li, P.; Lv, H.; Yang, C.; Peng, Q.; Zhu Y.; Guo, L.; Zhang, Y.; et al. Characterization of white tea metabolome: Comparison against green and black tea by a nontargeted metabolomics approach. *Food Res. Int.* **2017**, 96, 40-45. https://doi.org/10.1016/j.foodres.2017.03.028
36. Vliet, E.V.; Morath, S.; Eskes, C.; Linge, J.; Rappsilber, J.; Honegger, P.; Hartung, T.; Coecke, S. A novel in vitro metabolomics approach for neurotoxicity testing, proof of principle for methyl mercury chloride and caffeine. *NeuroToxicology* **2008**, 29, 1-12. https://doi.org/10.1016/j.neuro.2007.09.007
37. Chen, Y.; Ma, Z.; Shen, X.; Li, L.; Zhong, J.; Min, L.; Xu, L.; Li, H.; Zhang, J.; Dai, L. Serum Lipidomics profiling to identify biomarkers for non-small cell Lung cancer. *BioMed Res. Int*. **2018**, 2018, 5276240. https://doi.org/10.1155/2018/527624
38. Wang, X.; Zhang, H.; Song, Y.; Cong, P.; Li, Z.; Xu, J.; Xue, C. Comparative lipid profile analysis of four fish species by UPLC-Q-TOF-MS. *J. Agric. Food Chem.* **2019**, 67, 9423-9431. https://doi.org/10.1021/acs.jafc.9b03303
39. Wen, B.; Mei, Z.; Zeng, C.; Liu, S. MetaX: a flexible and comprehensive software for processing metabolomics data. *BMC bioinformatics* **2017**, 18, 183. https://doi.org/10.1186/s12859-017-1579-y
40. Yuan, M.; Breitkopf, S.B.; Yang, X.; Asara, J.M. A positive/negative ion-switching, targeted mass spectrometry-based metabolomics platform for bodily fluids, cells, and fresh and fixed tissue. *Nat. protoc.* **2012**, 7, 872-881. https://doi.org/10.1038/nprot.2012.024
41. Chong, J.; Xia, J. MetaboAnalystR: an R package for flexible and reproducible analysis of metabolomics data. *Bioinformatics* **2018**, 34, 4313-4314. https://doi.org/10.1093/bioinformatics/bty528

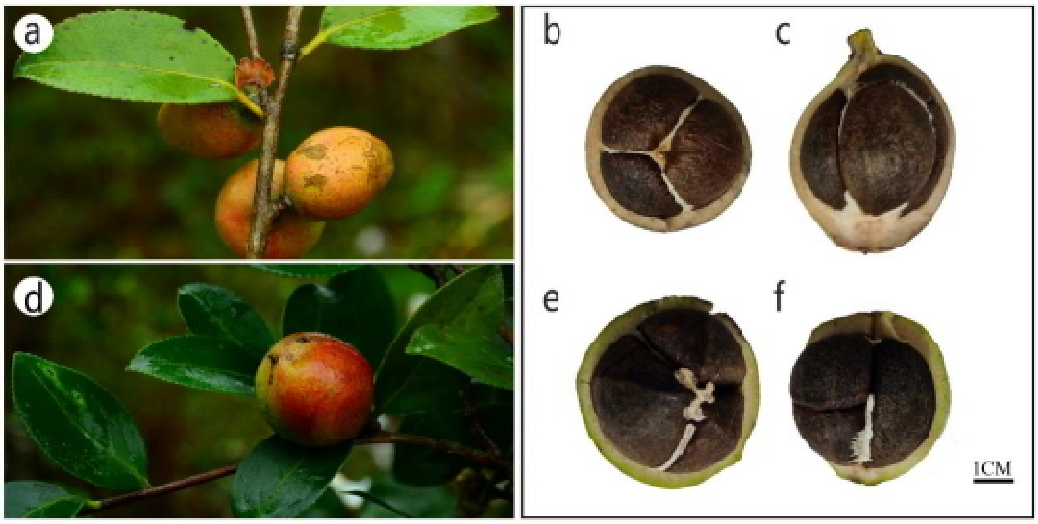

Fig. 1 Morphological observation of CL3 (a-c) and CL 53 (d-f). (a) Fresh fruits of CL3. (b) equatorial section of CL3 Fruit. (c) longitudinal section of CL3 Fruit. (d) Fresh fruits of CL53. (e) equatorial section of CL53 Fruit. (f) longitudinal section of CL53 Fruit.

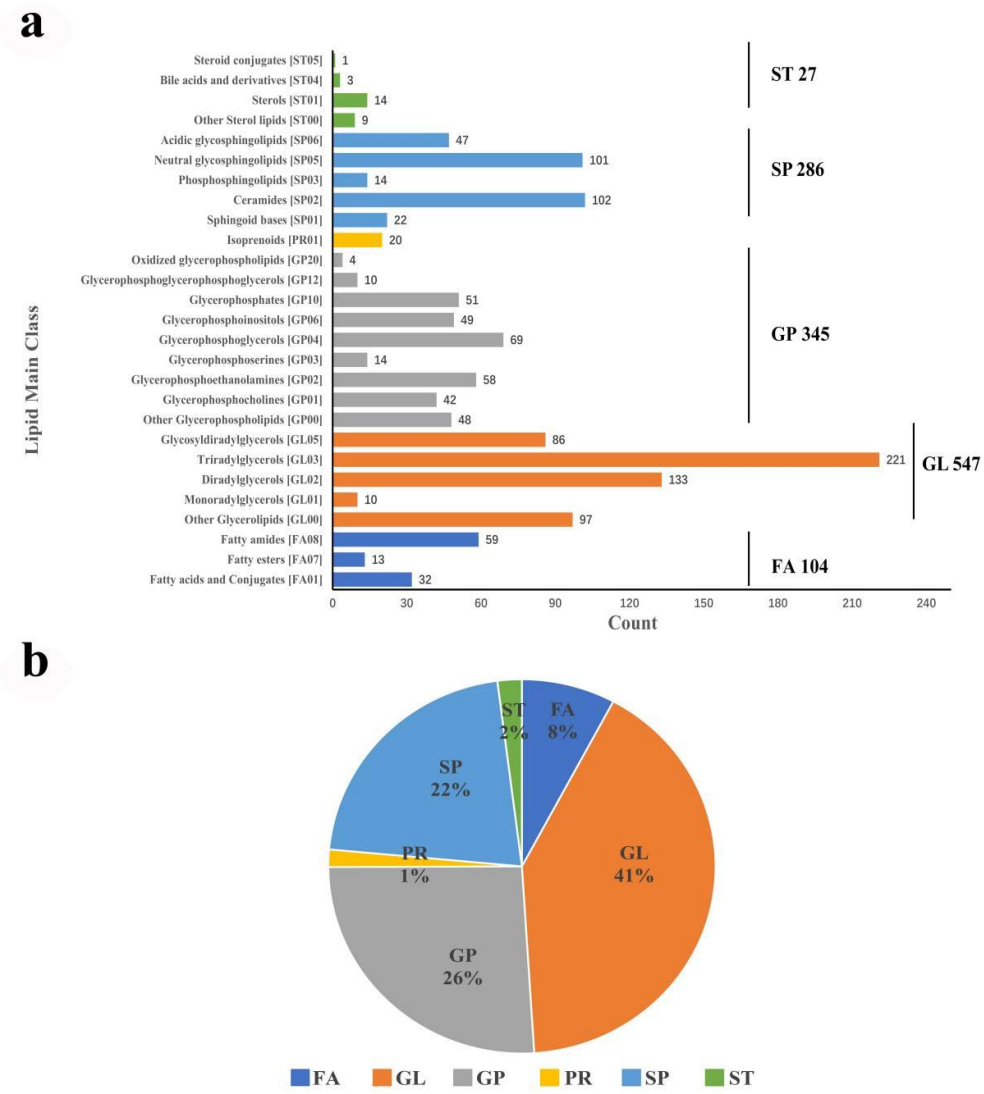

Fig. 2 Types and proportions of lipids in fresh kernels of mature *Camellia oleifera*. (a)The number of identified lipid main classes. (b) The percentage composition of lipid categories. FA, Fatty acyls; GL, Glycerolipids; GP, Glycerophospholipids; PR, Prenol lipids; SP, Sphingolipids; ST, Sterol Lipids.

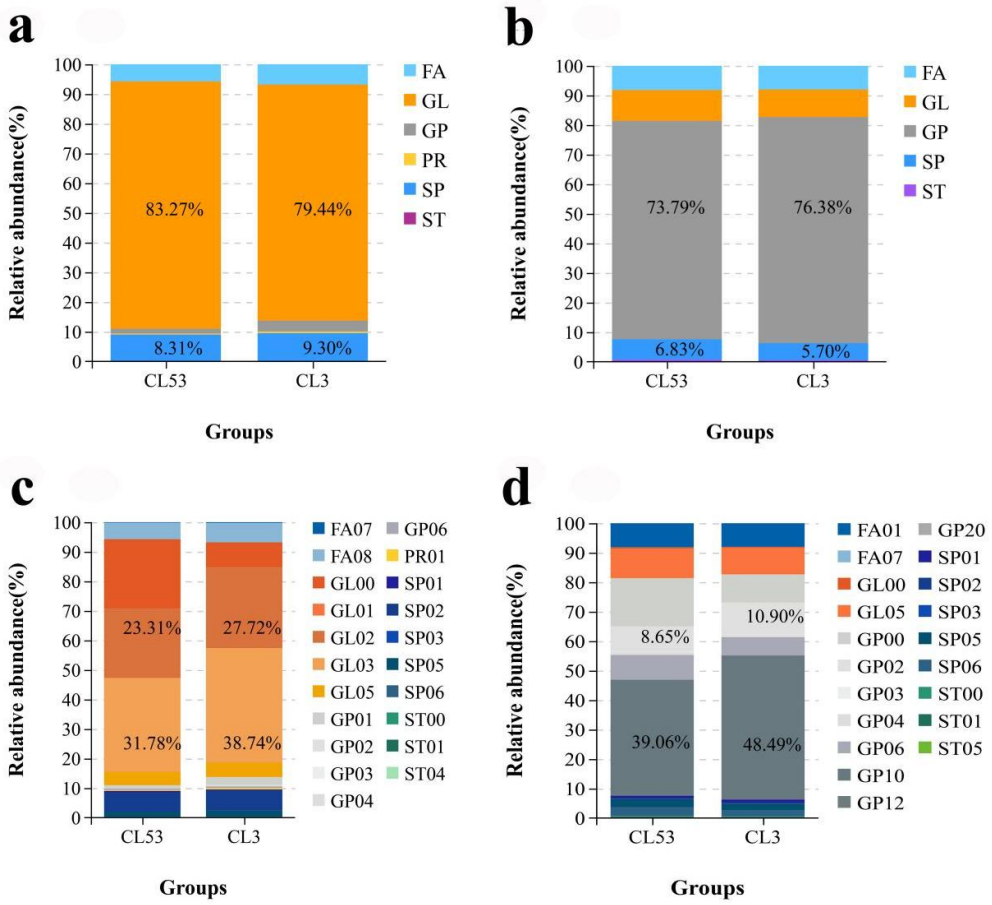

Fig. 3 The relative abundance of the relative concentration of the categories and main class lipids between C53 and CL3 samples. (a) Relative concentration of the categories in positive ion mode (NT-pos). (b) Relative concentration of the categories in negative ion mode (NT-neg). (c) Relative concentration of the main class lipids in positive ion mode (NT-pos). (d) Relative concentration of the main class lipids in negative ion mode(NT-neg).

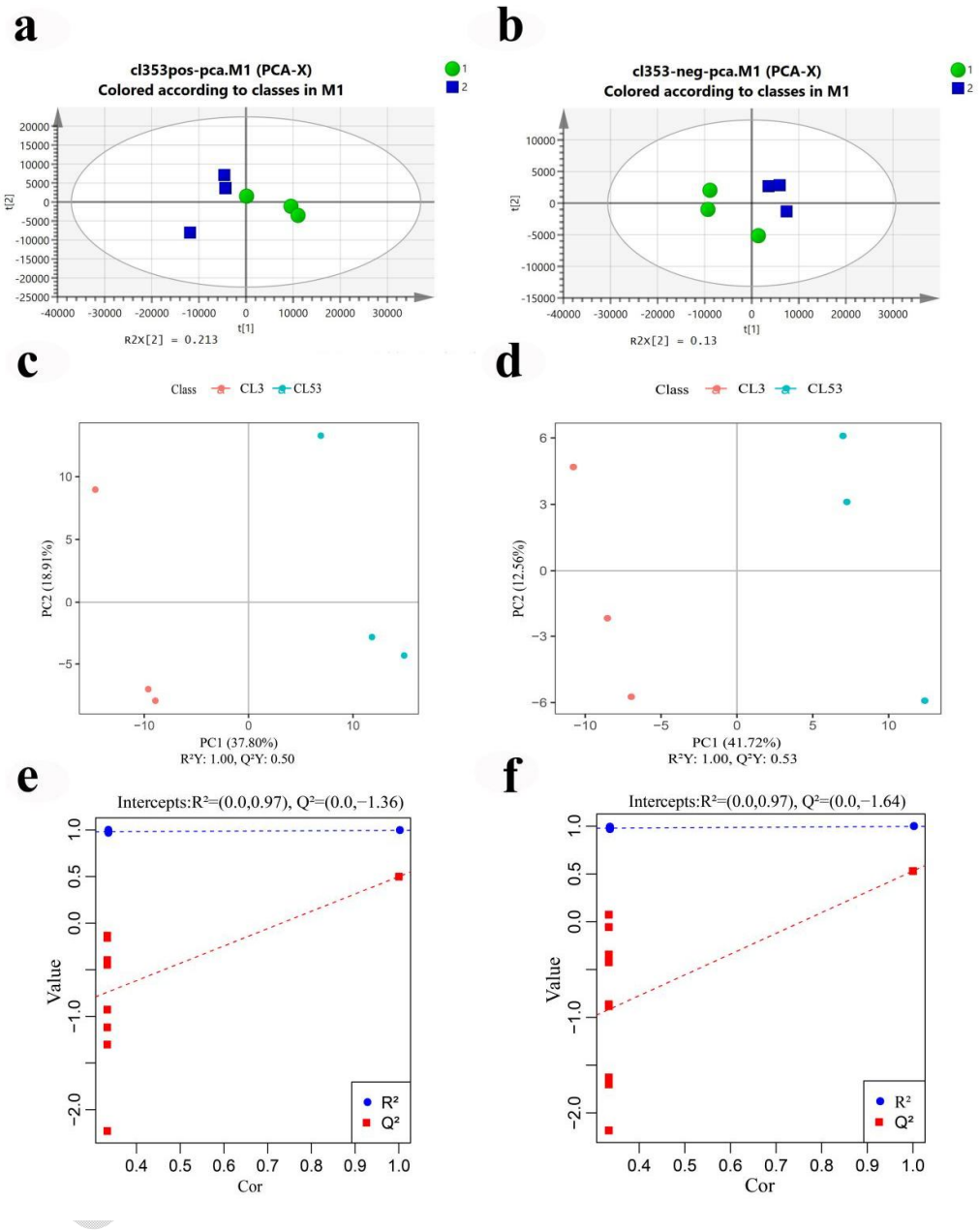

Fig. 4 Multivariate statistical analysis between CL3 and CL53. (a)PCA score charts based on NT-pos, R21[X]=0.581, R22[X]=0.213. (b) PCA score charts based on NT-neg, R21[X]=0.703, R22[X]=0.130. (c) PLS-DA score charts based on NT-pos. (d) PLS-DA score charts based on NT-neg. (e) PLS-DA permutation plot based on NT-pos. (f) PLS-DA permutation plot based on NT-neg. R^2Y, the interpretability of the model; Q^2Y the predictability of the model.

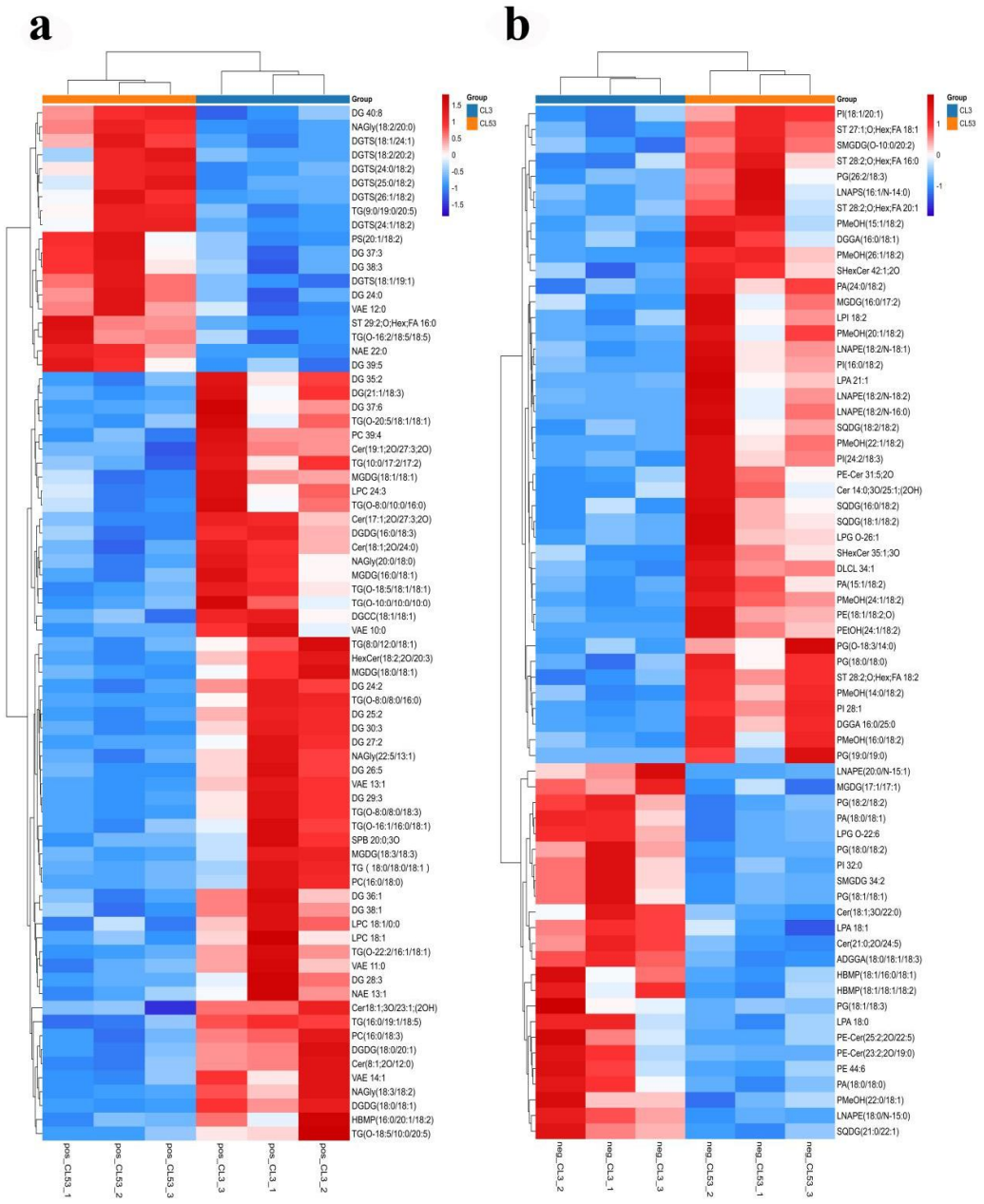

Fig. 5 Heat map analysis based on the relative concentration of 140 SDLs between CL3 and CL53.
(a) SDLs in NT-pos. (b) SDLs in NT-neg.

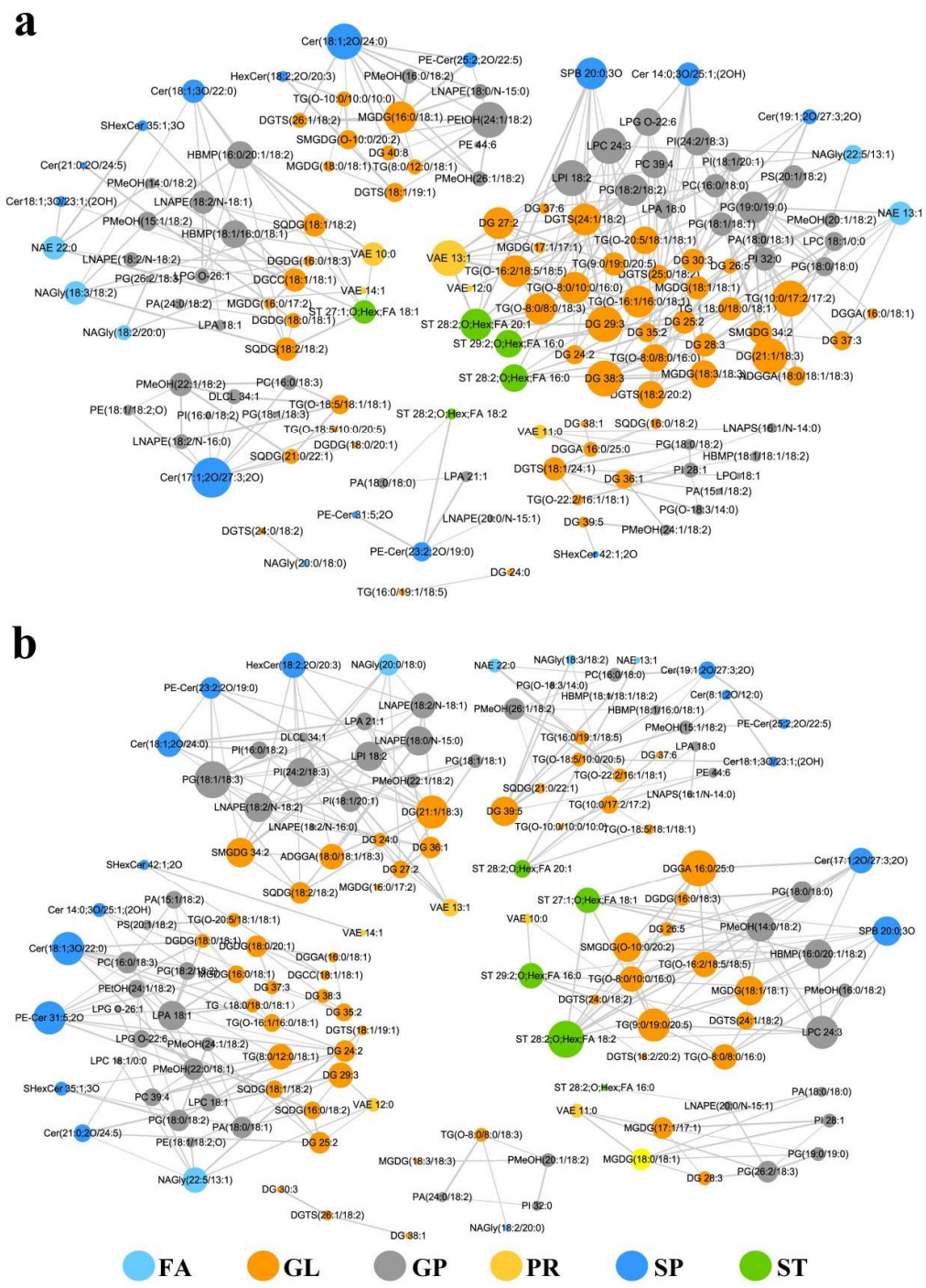

Fig. 6 Pearson correlation network (*P*-value<=0.05) of 140 SDLs in CL3 (a) and CL53 (b). Lipids species are color-coded as 6 categories. The size of node represents the level of relationship, the larger the node, the more SDLs associated. The width of edges represents the credibility of relevance (*P*-value), the wider the edge (the smaller the *P*-value), the higher the credibility of the correlation.

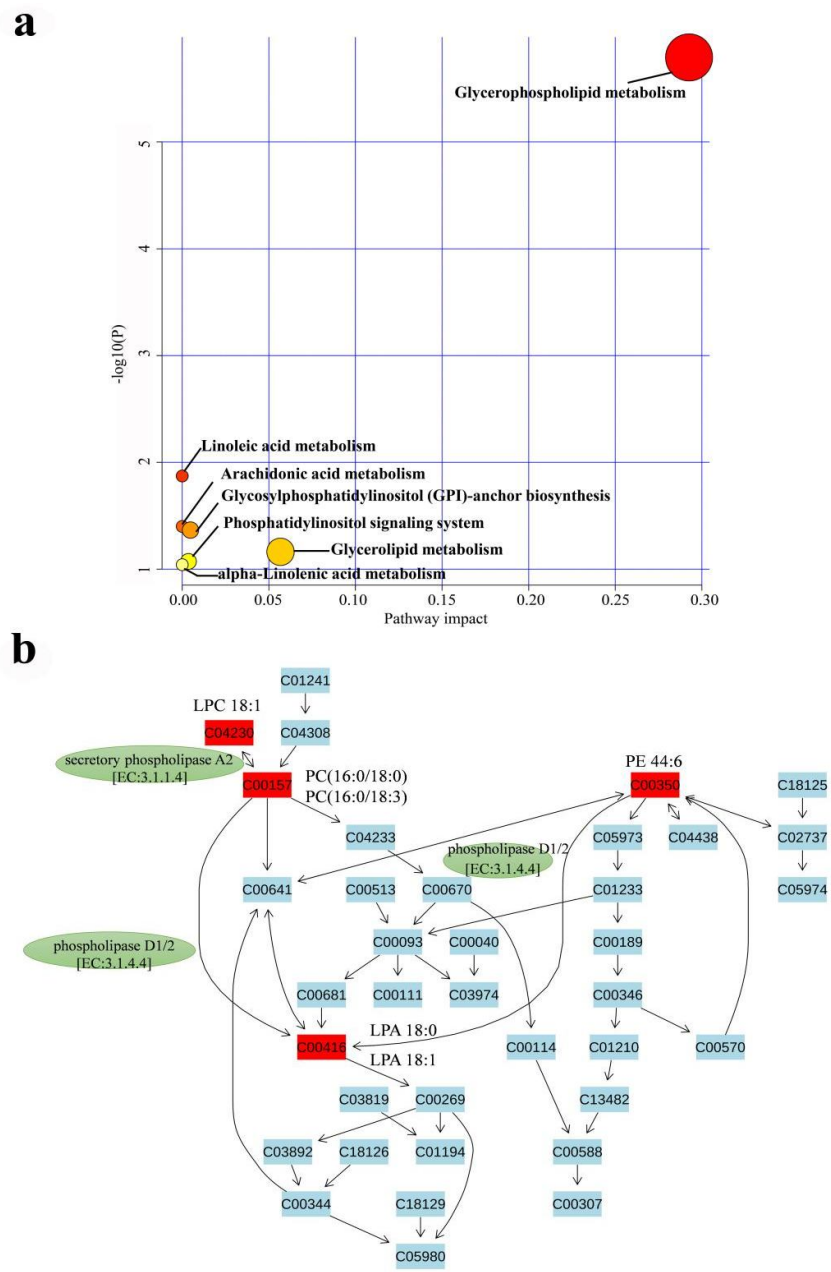

Fig.7 Analysis of 140 SDLs enrichment pathways and SDLs transition relationship in glycerophospholipid metabolism pathway. (a) Metabolomic view of the significant lipid biosynthetic pathways in CL3 and CL53. The X-axis represents the pathway impact, and the Y-axis represents the -ln *P*-value. Large sizes and dark colors represent major pathway enrichment and high pathway impact values, respectively. (b) Lipids transformation relationship in glycerophospholipid metabolism based on KEGG (https://www.kegg.jp/). The red rectangular boxes represent the id of enriched SDLs on KEGG databases; The green ellipse represents the enzyme that catalyzes this reaction.